

Kidney MR Elastography: Methods and Clinical Applications in Pediatric Kidney Transplantation

Suraj D. Serai, Ph.D.^{1,3}; Bernarda Viteri, M.D., MSTR^{2,3}; Hansel J. Otero, M.D.^{1,3}

¹Department of Radiology, Children's Hospital of Philadelphia, Philadelphia, PA, USA

²Division of Nephrology, Children's Hospital of Philadelphia, Philadelphia, PA, USA

³Perelman School of Medicine at the University of Pennsylvania, Philadelphia, PA, USA

Abstract

Magnetic resonance elastography (MRE) is well established for the evaluation of liver fibrosis. Our team now explores MRE as a promising non-invasive imaging technique for assessing the health of transplanted kidneys in children. This paper explains the principles, methodology, and clinical applications of MRE in evaluating kidney stiffness and its potential role in diagnosing and monitoring interstitial fibrosis and tubular atrophy (IFTA) in pediatric transplanted kidneys. Our study showed a correlation between kidney stiffness and histological fibrosis, with higher stiffness values observed in allografts with fibrosis compared to stable ones. This suggests that MRE could serve as a non-invasive tool for monitoring post-transplant kidney health, and thereby reduce the need for invasive biopsies and potentially enable more timely interventions.

Introduction

Dynamic elastography is a non-invasive imaging technique that uses shear waves to assess tissue stiffness by measuring its response to an applied force [1]. Magnetic resonance elastography (MRE) is a clinically validated, FDA-cleared method that provides a reliable estimate of soft tissue stiffness [2, 3], which is widely used in clinical practice for diagnosing and staging liver fibrosis [4, 5]. The technique works by applying low-frequency harmonic vibrations to a target tissue, then imaging the resulting propagating waves and processing the data to calculate mechanical parameters [6]. The result is a stiffness measurement displayed on an elastogram, a color-coded map that highlights variations in tissue stiffness and provides valuable objective quantitative information that helps identify disease presence and progression [7].

Kidney MRE

While a healthy kidney is typically soft and pliable, a diseased kidney may become stiffer due to inflammation, scarring, or fibrosis. Since the mechanical properties of renal tissues change with underlying pathologies, MRE can be used to spatially assess tissue stiffness and would potentially allow doctors to assess the health of the kidneys [6, 7]. For example, kidney MRE could assist in the management of patients with chronic kidney disease (CKD) to monitor progression. In the case of transplanted kidneys, MRE could help monitor for signs of rejection or other complications. MRE generates a color-coded map called an elastogram. The desired output is to measure the stiffness value from the elastogram. The elastogram that is generated from the acquired images indicates areas of tissue stiffness and can give objective quantitative information about the presence of disease.

Methods

MRE utilizes low-frequency sound waves to generate shear waves in the tissue or organ of interest (in this case, the kidneys). In the commercial version of MRE provided by Resoundant Inc. (Rochester, MN, USA) and used on clinical MRI scanners, mechanical waves are produced by an “active driver” that is positioned outside the scanner room and controlled by the scanner. The pressure waves are transmitted through a plastic tube to a “passive driver” placed on the patient’s body. While the original passive drivers were flat disks, they are now being replaced with soft, flexible models that adapt to the shape of the body. The passive driver is held in place by an elastic band. Patients can feel the vibration applied by the driver, but it is generally not uncomfortable.

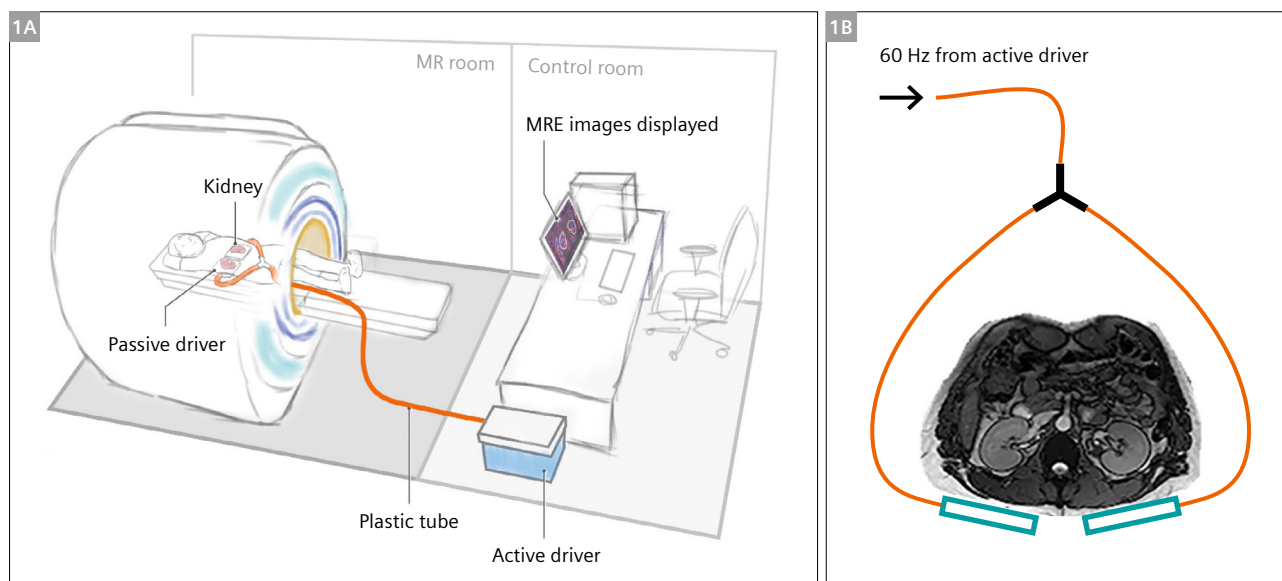
Patient setup for kidney MRE

Instead of the single circular passive driver that is typically used for the liver, a Y-shaped splitter is used to connect two passive drivers placed on the back of the patient. The drivers should be positioned over the approximate location of the left and right kidneys (Fig. 1). For patients with single allograft kidney, a single passive driver is used.

Implementation of MRE

MRE data is acquired using special gradient-recalled echo (GRE) or spin-echo echo-planar imaging (SE-EPI) sequences. Both sequences work well on 1.5T systems, but the SE-EPI sequence has proven effective in reducing technical failures due to iron overload [8]. The SE-EPI MRE sequence is also recommended for 3T MRI systems, where T2* decay in the liver is more rapid [9].

The MRE implementation that is now widely used in clinical practice for evaluation of liver disease acquires individual cross-sectional images of propagating shear waves. The driver system is designed to generate shear waves in the liver that propagate mainly in directions parallel with the x-y plane and therefore can be accurately recorded with transverse images. In the standard liver MRE protocol, four transverse sections of the liver are acquired with through-plane motion encoding. The wave images are individually processed with a 2D inversion algorithm to generate elastograms. This approach, called 2D MRE, has been extensively validated and shown to efficiently provide reliable liver stiffness measurements. It is regarded as the most accurate non-invasive imaging-based method for detecting and staging liver fibrosis.



1 (1A) Kidney MRE passive driver positioning. The driver is positioned posteriorly so that it is relatively close to the kidney from the dorsal side. (1B) A Y-shaped splitter is used to position two paddles in parallel under both kidneys. Figure adapted and modified from [8].

Today, 2D MRE is widely available on clinical MRI scanners and can be relatively easily translated to the kidney [8]. A detailed protocol for kidney MRE acquisition is provided in Table 1.

Method	MRE with 2D motion encoding	MRE with 3D motion encoding
Pulse sequence	2D SE-EPI	3D SE-EPI
Matrix size	100 × 100	96 × 96
Echo time, TE (msec)	35	36
Repetition time, TR (msec)	1200	4200
Bandwidth (Hz/px)	2174	2380
Slice thickness (mm)	8	3.6
Distance factor	25%	18%
No. of slices	4	14
No. of phases	4	3
Axis of MEG	Z	X, Y, and Z
Driver frequency (Hz)	60	60
Acceleration	GRAPPA	GRAPPA
Acceleration factor	2	3
No. of breath-holds	1	5
Imaging time (min: sec)	0:13	1:27

Table 1: Pulse sequence parameters for 2D and 3D MRE¹.

SE-EPI: spin-echo echo-planar imaging; 2D: two dimensional; 3D: three dimensional; MRE: magnetic resonance elastography; MEG: motion encoding gradients; msec: milliseconds; mm: millimeters; Hz: hertz; mT/m: millitesla/meter; Px: pixel; min: minutes; sec: seconds

3D MRE¹

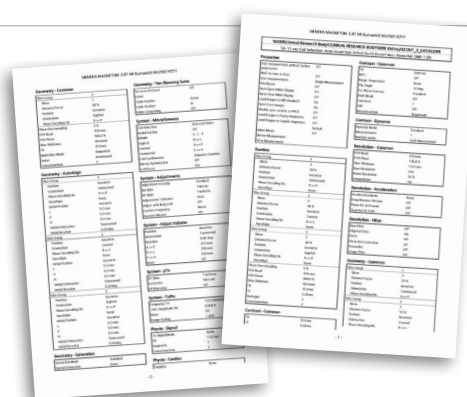
When MRE is used to evaluate the kidneys and other organs, the pattern of wave propagation is often much more complex than in the liver application. This can be addressed with an implementation of MRE that encodes the wavefield in all three dimensions. This implementation is known as 3D MRE, and includes encoding for cyclic motion in X, Y, and Z directions rather than just in one direction. It is important not to confuse 3D MRE with 3D volumetric imaging in the common meaning. The 3D MRE data are processed with a special 3D MRE inversion algorithm that considers wave propagation in all directions in 3D space. By capturing and processing wave data throughout a volume and in all directions of propagation, and by measuring cyclic motion in all directions, the 3D vector MRE technique can provide a more accurate measurement of tissue stiffness in complex anatomy. Moreover, 3D vector MRE processing can yield additional biomarkers such as the individual components of the complex shear modulus [11].

Given the kidney's small size and relatively deep location in comparison to the liver, accurate and reproducible stiffness measurement may benefit from 3D analysis of wave field data. Due to its enhanced accuracy and ability to measure wave motion in all three directions, 3D MRE is expected to outperform 2D MRE in kidney assessment.

Shear stiffness, (G^*), also called the magnitude of the complex shear modulus, $|G^*| = \sqrt{((G')^2 + (G'')^2)}$, is the commonly used MRE parameter; it reflects both elastic and viscous (or damping) elements of tissue stiffness. 3D MRE evaluates additional mechanical properties related

¹3D MRE is work in progress. It is a joint development of Mayo Clinic, Rochester, MN, USA; Resoundant Inc., Rochester, MN, USA and Siemens Healthineers. The application is currently under development and is not for sale in the U.S. and in other countries. Its future availability cannot be ensured.

To download the **exar.1** file and the PDF, please visit us at www.magnetomworld.siemens-healthineers.com and go to **Clinical Corner > Protocols**



to the dynamic aspects of stiffness, including storage modulus (G' , elastic behavior), loss modulus (G'' , viscous behavior), and damping ratio (loss modulus divided by $2 \times$ storage modulus). Preclinical and clinical studies suggest that these parameters are differentially impacted by fibrosis and inflammation [9, 10]. Early data indicate that the extra parameters measured by 3D MRE provide a more comprehensive evaluation than 2D MRE, which focuses solely on stiffness.

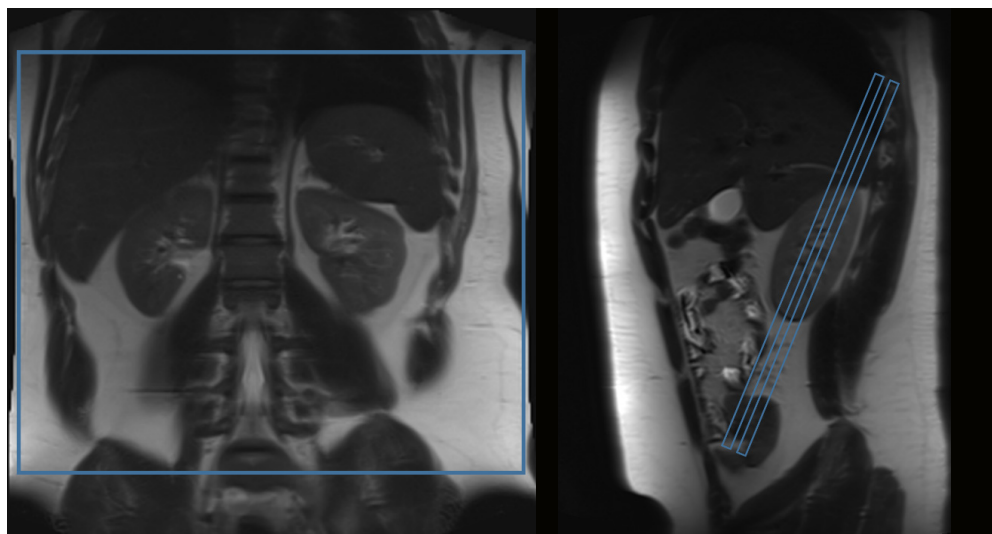
Image acquisition

First, scout images: 3 to 5 slices in all three orthogonal planes are obtained in a single breath-hold during end-expiration to match MRE acquisition. MRE slices are acquired in an oblique coronal plane aligned to the long axis of the kidneys (Fig. 2). For our study, both 2D and a 3D MRE acquisition sequences were run on the same scanner and in the same imaging session. The MRE acquisitions were performed back-to-back. The spatial resolution,

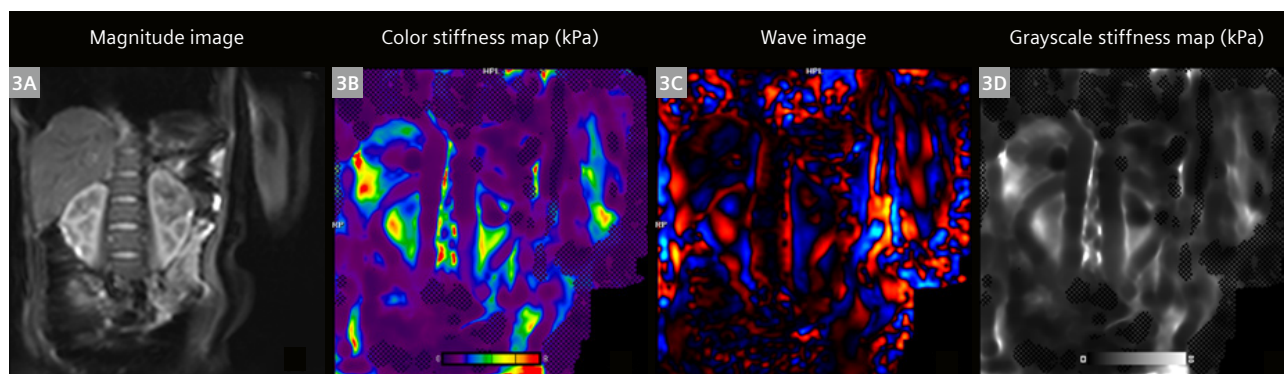
bandwidth, and motion-encoding gradient frequency were optimized to keep the imaging time to approximately 15 seconds per breath-hold. For the 2D SE-EPI image acquisition, all data are acquired in a single breath-hold at end-expiration (Fig. 3). Pulse sequence parameters for 2D and 3D SE-MRE are detailed in Table 1.

Stiffness measurement

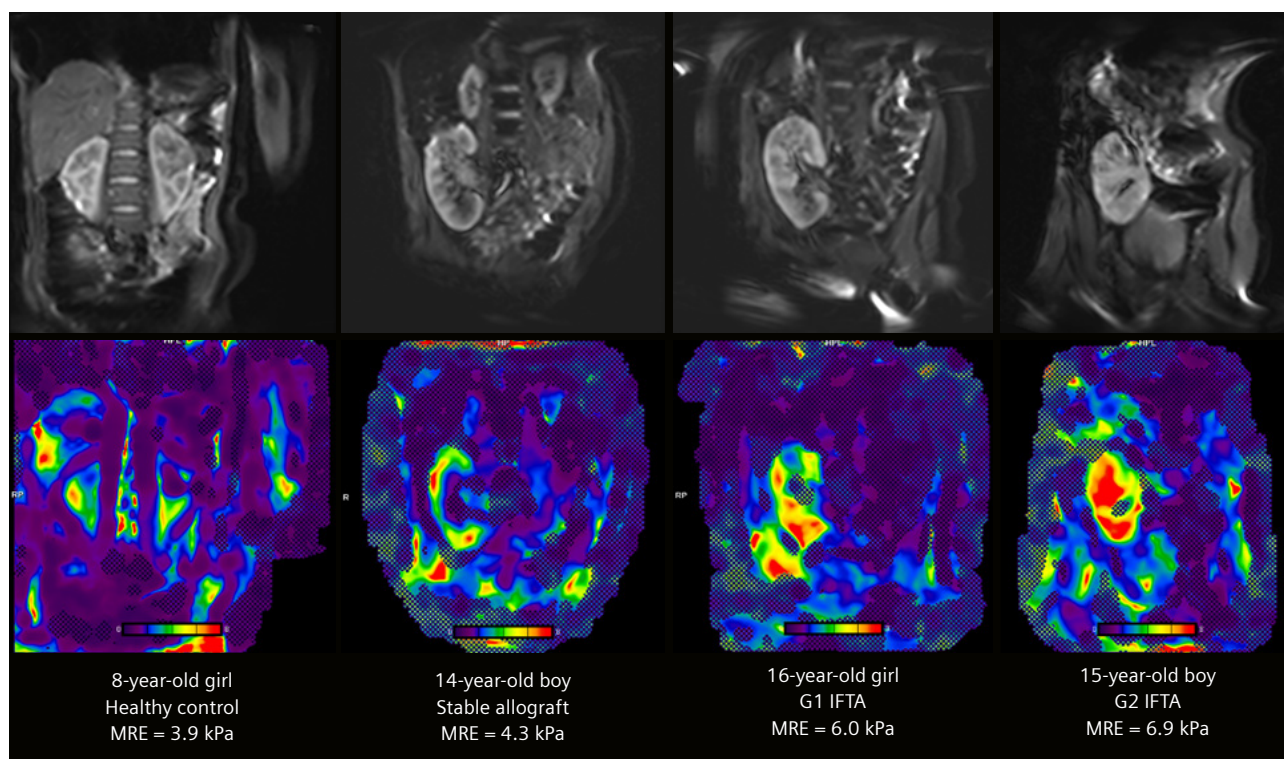
Analogous to liver MRE, the stiffness maps and the 95% confidence maps are generated on the scanner. All MRE images must be reviewed for any breathing or motion artifacts that could render the images undiagnostic. Regions of interest (ROI) for measurement of stiffness are drawn within the regions bound by the confidence maps to include as much of the kidney parenchyma as possible, staying within the outer kidney capsule. A weighted mean shear stiffness is calculated. For 3D MRE, ROIs are carefully matched to record measurements of stiffness, storage modulus, and loss modulus.



2 T2W coronal and sagittal slices showing the MRE slice setup.



3 Representative MRE images (2D SE-EPI) of an 8-year-old girl recruited as a healthy control. Mean kidney stiffness was measured as 3.9 kPa.



4 Representative MRE (2D SE-EPI) images of an 8-year-old girl recruited as a healthy control; a 14-year-old boy with stable allograft; a 16-year-old girl with Grade 1 IFTA; and a 15-year-old boy with Grade 2 IFTA. Mean kidney stiffness was measured as 3.9 kPa, 4.3 kPa, 6.0 kPa, and 6.9 kPa, respectively.

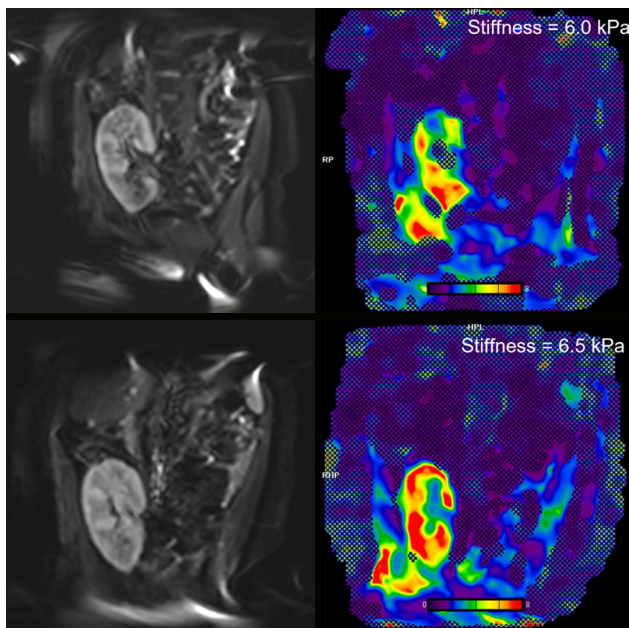
Clinical applications in children post-kidney transplant

MR imaging can characterize kidney structures. However, biopsies remain the primary method for diagnosing kidney pathologies, despite their associated risks and complications. A non-invasive method such as MRE can help identify and monitor kidney parenchymal abnormalities with the potential to spare or at least space out the need for biopsies. In patients with a transplanted kidney, interstitial fibrosis and tubular atrophy (IFTA) are major histopathologic factors in kidney allograft failure. IFTA progresses in two phases: The early phase, within the first year post-transplant, is characterized by fibrogenesis and tubulointerstitial injury due to ischemic or immunological damage. The late phase, beyond the first year, involves severe graft injury, including fibrosis, tubular atrophy, glomerulosclerosis, and arteriolar hyalinosis, leading to irreversible graft loss. Currently, percutaneous biopsy remains the gold standard for diagnosing and evaluating IFTA.

In our study, we observed a positive correlation between kidney elasticity and histological fibrosis, with stiffness values generally being higher in fibrosed allografts compared to stable ones and also compared to normal native kidneys [8]. Mean kidney stiffness was higher for IFTA allografts (5.6 kPa) than stable allografts (4.4 kPa) and controls (3.6 kPa) (Fig. 4) [8].

Discussion

Application of MRE for non-invasive evaluation of renal fibrosis has great potential for non-invasive assessment in patients with kidney transplant. However, further development and testing of these applications are necessary, primarily to validate the measurement against gold-standard invasive methods, to establish the discriminatory limits of MRE, and to better understand the physiology and pathophysiology of the observed changes in stiffness. On a technical note, MRE in patients with kidney transplants is relatively easy to perform, as the graft is usually located



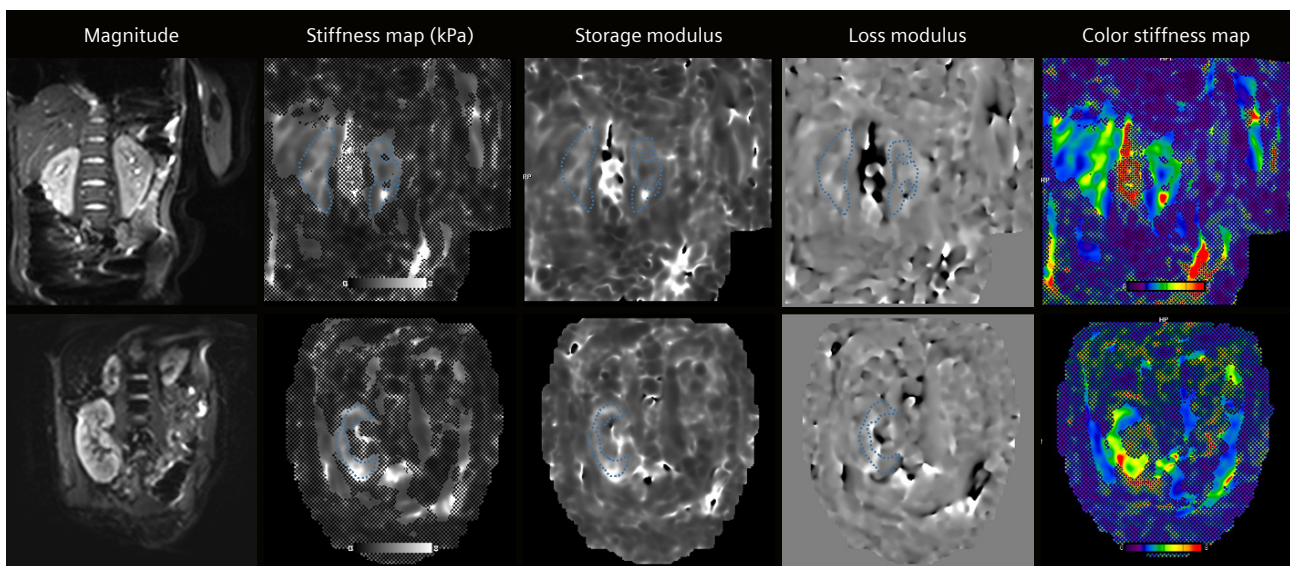
5 Longitudinal scan of a 16-year-old girl with Grade 1 IFTA. A mean kidney stiffness of 6.0 kPa was measured at baseline, and an increase in stiffness is seen on the scan performed 18 months later.

in the lower abdomen, where it is subject to less movement from respiration, and is closer to the skin surface, which would facilitate relatively easier transmission of the shear wave (Fig. 5). Our preliminary results showed that MRE has the potential to be used as a non-invasive tool for quantitative measurements of the degree of fibrosis in renal allografts with a strong correlation with histopathology [8]. We think this is because the diffuse interstitial fibrosis increases tissue stiffness similar to the increased stiffness in liver fibrosis. Moreover, MRE has shown that it can help discriminate between the different IFTA groups [8].

While 3D MRE offers some advantages in robustness, patient comfort, and additional tissue data (Fig. 6), 2D MRE, which is more widely available, still holds significant potential in the basic application of detecting IFTA in patients with kidney transplant.

Conclusion

Kidney MRE shows promise in detecting low-grade IFTA in allografts. If clinically implemented, elastography would be useful for early detection of IFTA in renal transplants.



6 In addition to stiffness maps, 3D MRE allows the generation of storage modulus, loss modulus, and damping ratio. ROIs were carefully matched to record measurements. The top row shows representative images of 3D MRE on the same 8-year-old girl (stiffness = 3.8 kPa; storage modulus = 3.6 kPa; loss modulus = 2.0 kPa; damping ratio = 0.2). The bottom row shows representative images of 3D MRE on the same 14-year-old boy with stable allograft (stiffness = 4.6 kPa; storage modulus = 4.2 kPa; loss modulus = 0.85 kPa; damping ratio = 0.1).

This would individualize the need for immunosuppression therapy with the added benefit of reducing the need for invasive biopsies.

Acknowledgments

We thank Robert Sellers and Bradley Bolster Jr. at Siemens Healthineers USA for providing access to the prototype 3D MRE acquisition sequence. We thank Richard L. Ehman and Meng Yin at Mayo Clinic for their support with MRE.

Funding

This study was partly funded by the National Institute of Diabetes and Digestive and Kidney Diseases of the National Institutes of Health under grant number K23DK131331.

References

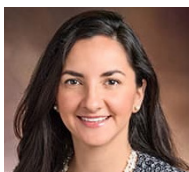
- 1 Serai SD, Trout AT, Sirlin CB. Elastography to assess the stage of liver fibrosis in children: Concepts, opportunities, and challenges. *Clin Liver Dis (Hoboken)*. 2017;9(1):5–10.
- 2 Towbin AJ, Serai SD, Podberesky DJ. Magnetic resonance imaging of the pediatric liver: imaging of steatosis, iron deposition, and fibrosis. *Magn Reson Imaging Clin N Am*. 2013;21(4):669–80.
- 3 Serai SD, Towbin AJ, Podberesky DJ. Pediatric liver MR elastography. *Dig Dis Sci*. 2012;57(10):2713–9.
- 4 Joshi M, Dillman JR, Towbin AJ, Serai SD, Trout AT. MR elastography: high rate of technical success in pediatric and young adult patients. *Pediatr Radiol*. 2017;47(7):838–843.
- 5 Serai SD, Obuchowski NA, Venkatesh SK, Sirlin CB, Miller FH, Ashton E, et al. Repeatability of MR Elastography of Liver: A Meta-Analysis. *Radiology*. 2017;285(1):92–100.
- 6 Serai SD, Yin M. MR Elastography of the Abdomen: Basic Concepts. *Methods Mol Biol*. 2021;2216:301–323.
- 7 Serai SD, Yin M. MR Elastography of the Abdomen: Experimental Protocols. *Methods Mol Biol*. 2021;2216:519–546.
- 8 Elsingery MM, Viteri B, Otero HJ, Bhatti T, Morales T, Roberts TPL, et al. Imaging fibrosis in pediatric kidney transplantation: A pilot study. *Pediatr Transplant*. 2023;27(5):e14540.
- 9 Yin M, Glaser KJ, Manduca A, Mounajjed T, Malhi H, Simonetto DA, et al. Distinguishing between Hepatic Inflammation and Fibrosis with MR Elastography. *Radiology*. 2017;284(3):694–705.
- 10 Qu Y, Middleton MS, Loomba R, Glaser KJ, Chen J, Hooker JC, et al. Magnetic resonance elastography biomarkers for detection of histologic alterations in nonalcoholic fatty liver disease in the absence of fibrosis. *Eur Radiol*. 2021;31(11):8408–8419.

Contact

Suraj D. Serai, Ph.D.
Children's Hospital of Philadelphia
3401 Civic Center Blvd.
Philadelphia, PA 19104
USA
serais@chop.edu



Suraj D. Serai, PhD



Bernarda Viteri, MD



Hansel J. Otero, MD